Electric Field Simulations of High Voltage DC Extruded Cable Systems

Frank Mauseth and Hallvar Haugdal
Norwegian University of Science and Technology
Dept. of Electric Power Engineering
O.S. Bragstads Plass 2E
NO-7491 Trondheim, Norway

This article describes some of the most important aspects of electric field calculations and distributions in polymeric HVDC cables and their accessories, mainly focusing on interfaces and the influence of temperature.

Introduction

The market for high voltage direct current (HVDC) transmission systems has increased dramatically the last few decades. This is mainly due to the economic, electrical and environmental advantages for bulk power transmission over long distances. Also, in some cases, such as for long subsea cable links, HVDC is the only option. HVDC cables has traditionally used oil-paper for insulation with the most common type being the mass-impregnated non-draining (MIND) cable. The oil or mass-impregnated cables has for a century shown to have a very high reliability and are currently used for voltages and power ratings up to 525 kV and about 1 GW. Today, it is still the preferred technology for the highest voltage levels [1]. However, in the last two decades, extruded polymeric insulation has become more popular and the highest voltage level currently installed is ±320 kV used for grid interconnections and for offshore wind farms. HVDC cable systems using cross-linked polyethylene (XLPE) are available for voltages up to ±600 kV and 3 GW and polypropylene based for ±600 kV and 3.5 GW.

Extruded HVDC cable systems offer some advantages compared to oil-paper solutions; such as lower costs, easier and faster jointing, no oil-leakage and higher conductor temperature. However, there are also disadvantages such as limited service experience and challenges related to trapped space charge within the insulation. The existence of space charge poses a potential threat to the reliability of the operation of HVDC cables and their accessories. Trapped space charge can give rise to high local field stresses, which might initiate or cause breakdown, especially in interfaces and with temperature gradients, and during rapid grounding due to faults or polarity reversals [2],[3].

Thus, quantitative knowledge of the electric field distribution within a polymeric HVDC system is essential when designing a cable and its accessories. A HVDC system will not only experience a DC stress, but also AC stress due to lightning and switching impulses. In addition, a combination of DC and AC voltage stresses can be experienced during the lifetime of the cable system.

In this article, the role of interfaces and temperature gradient is illustrated through three examples; 1) Maxwell-Wagner capacitor with a two-layered structure, 2) HVDC cable and 3) a simplified cable joint.

Electric field stress in a HVDC system

In a HVAC cable, the calculation of the electric field stress is relatively straightforward as the electric field distribution at AC is governed by the permittivity ε of the insulation material, cable geometry, and the voltage applied. Since the permittivity can be considered constant at service temperatures, the electric field distribution can be considered unaffected by any loading situation of the cable [4]. The electric field distribution at DC is more

complex as the field distribution depends on the permittivity, conductivity σ, geometry, loading and applied voltage. Generally, the conductivity can be given by the empirical formula [5]:

$$\sigma(T,E) = \sigma_0 e^{\alpha T + \beta E} \qquad (1)$$

where σ_0 is the conductivity at 0 °C and an electric field strength of 0 kV/mm, and α and β is the temperature and field dependency, respectively.

The various electric field stages during HVDC voltage application can be illustrated by Figure 1. Considering a HVDC cable free of space charge and no temperature gradient across the insulation when turning on the voltage, the field distribution will initially be governed by the permittivity and geometry only. Then, a change from capacitive to resistive field distribution will take place before a DC state is established. During this period, the field distribution will be time dependent, and the time before the DC state is reached can take from minutes to days, depending on the material properties and loading situation. When the voltage is switched off, any remaining space charge in the insulation system will generate an electric field. In the case of a polarity reversal, the same space charge can severely affect the field distribution resulting in a high local electric field strength that can lead to degradation of the insulation and eventually cause breakdown. This is especially the case for larger temperature gradients and at interfaces. Also, the large time constants involved in such systems and a loading situation changing with time will likely lead to an electric field that never reaches a true steady state condition.

The continuity equation, derived from Gauss' law and Ampère's law, states that if there is an inequality in the current density, in or out of a region or volume, charge is accumulated. Thus,

$$\nabla \cdot J + \frac{\partial \rho}{\partial t} = 0 \qquad (2)$$

where J is the current density and ρ is the space charge. Using Gauss' law, the electric field E associated with the accumulated charge can be found by:

$$\nabla \cdot D = \nabla \cdot \varepsilon E = \rho \Leftrightarrow \nabla \cdot E = \frac{\rho}{\varepsilon} \qquad (3)$$

and the field distribution will be the sum of two contributions; the Laplacian capacitive field and the space charge induced field.
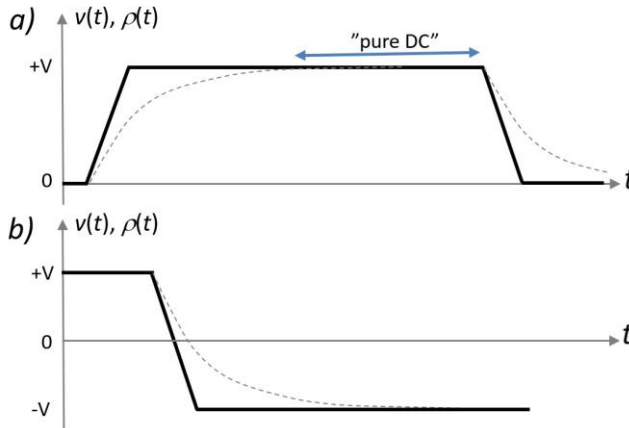
Figure 1. Voltage and space charge (dotted line) build-up/decay when a) turning voltage on and off and b) at polarity reversal [4].

Electric Field Simulations – Modelling and Results

Maxwell-Wagner capacitor

Consider a parallel plane capacitor with two layers of insulation, each with a thickness $d_1 = d_2 = 1$ mm, with relative permittivities $\varepsilon_1 = 2$ and $\varepsilon_2 = 4$ and conductivities $\sigma_1 = 4\cdot10^{-15}$ S/m and $\sigma_2 = 2\cdot10^{-15}$ S/m. When applying a DC voltage, interfacial charge builds up at the interface that can be found from (3). At the moment of switching on the voltage, the electric field in the layers is given by the capacitive distribution, before the change to a resistive field distribution takes place. The time constant for the transition can be calculated [5] from:

$$\tau \approx \frac{d_2\varepsilon_1 + d_1\varepsilon_2}{d_2\sigma_1 + d_1\sigma_2} \qquad (4)$$

resulting in a time constant of around 8850 sec. (ca. 2.5 h) for this particular configuration and the steady state DC field distribution can be found using Ohm's law:

$$J = \sigma E \qquad (5)$$

The field distribution from capacitive to resistive can be calculated using finite element method (FEM) software. After establishing a steady state DC field, two cases are of particular interest here; the effect of turning the voltage off and the effect of polarity reversal on the field distribution in the two layers and the interfacial charge build-up and decay. Initially, when applying a 30 kV step voltage to the insulation configuration, the field is determined by the permittivities, resulting in a field strength of 20 and 10 kV/mm in layer 1 and 2, respectively (Figure 2). As the transition to the resistive field distribution takes place, interfacial charge accumulates at the interface between the two layers, as shown in Figure 3. After 15 h of voltage application, the voltage is switched off and the sample is short-circuited. The presence of charge at the interface causes induced fields of equal magnitude but opposite directions in the two layers, that will slowly decay towards zero. Also for charge decay, it can take hours or even days, depending on the material properties and geometry, to remove all the built-up charge. This can give unfortunate electric field situations with high local fields if for example a voltage of opposite polarity is applied shortly after switching the voltage off.
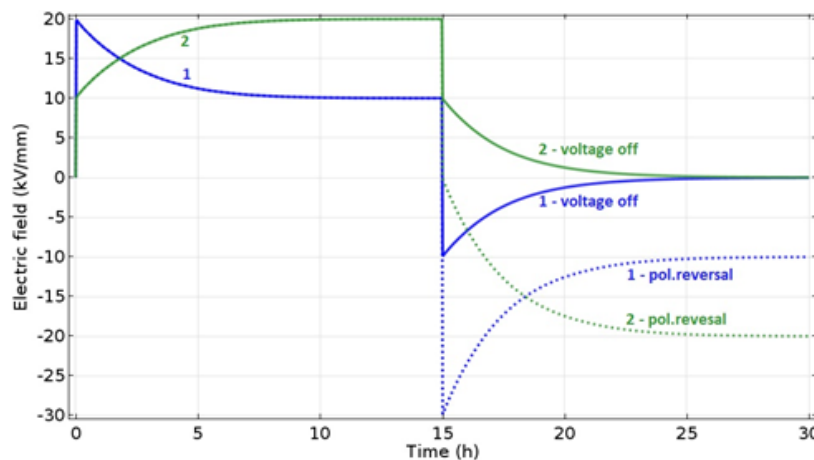
Figure 2. Electric field in the two layers vs time in the Maxwell-Wagner capacitor when switching on a 30 kV DC step voltage at $t = 0$ and switching the voltage off at $t = 15$ h or applying a polarity reversal at $t = 15$ h (dotted lines).

In the case of a polarity reversal, any charge present can lead to a very high local field that might initiate or cause breakdown. As shown by the dotted lines in Figure 2, directly after polarity reversal when switching from +30 to -30 kV at $t = 15$ h, the electric fields of layers 1 and 2 are 30 and 0 kV/mm, respectively, before a new steady state DC

distribution is established with the same field strengths as just before the polarity reversal, but in the opposite direction.

In addition, interfacial space charge injection can occur around inclusions and contaminations that usually have a much higher conductivity compared to the surrounding insulation material. Also, when the electric field exceeds a certain limit, space charge build-up can occur [6]. This space charge can result in degradation and electrical treeing under abrupt grounding or voltage-off [2].
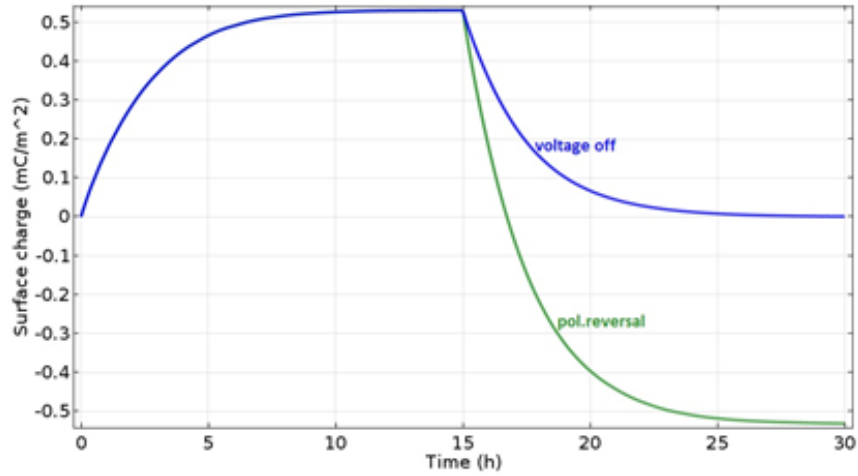
Figure 3. Interfacial charge build-up when switching on a DC step voltage and off (blue) or performing a polarity reversal (green) after 15 h of voltage application.

HVDC cable model - influence of temperature gradient

As interfacial and space charge are generated as the ratio ε/σ varies, the temperature distribution within a loaded 500 kV HVDC cable will cause accumulation of space charge. In this case, an XLPE insulated HVDC cable is studied, with conductivity

$$\sigma(T,E) = 3 \cdot 10^{-16} e^{0.05T + 0.03E} \ \left[\mathrm{S/m}\right] \qquad (6)$$

where T is given in °C and E in kV/mm and XLPE with a relative permittivity of 2.3. The cable has an insulation thickness of 23 mm with an inner radius of 34.5 mm and an outer radius of 57.5 mm. In addition, there is a semi-conductor of 1 mm thickness on both sides. The temperature at the outer semiconductor layer was set to 20 °C while varying the temperature at the inner semiconductor layer to create a temperature gradient ΔT varying from 0 to 20 °C.

The cable can be analysed in a cylindrical coordinate system, such that the geometry is independent of the z and ϕ coordinates. This allows the cable to be modelled as a one-dimensional line with axisymmetric field equations. The problem is solved using COMSOL Multiphysics®. First, the temperature distribution is determined, where variation with load is not taken into account, by solving a static heat transfer problem. Then, the electric potential is solved by performing a simulation in time, with boundary conditions for voltage and material properties as stated above.

Regardless of the temperature gradient over the insulation, the field distribution will be capacitive and similar for all cases when turning on the voltage. Due to the temperature varying radially throughout the insulation and the fact that the conductivity also is field dependent, the ratio of ε/σ will vary through the insulation at different rates for all cases studied here and result in a build-up of space charge. This is illustrated in Figure 4, where the steady-state DC field distribution for for ΔT = 0, 10 and 20 °C is shown for both a field independent and dependent conductivity.
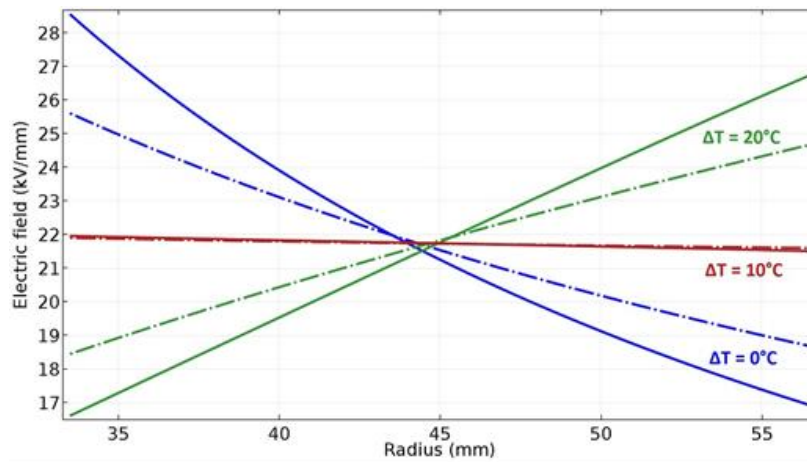
Figure 4. DC field distribution versus temperature gradient ΔT over the insulation without (solid line) and with (broken lines) field dependency of the conductivity (β = 0.03 mm/kV).

A temperature gradient gives, as expected, an increase in the electric field stress in the colder regions with a corresponding build-up of space charge throughout the insulation as shown in Figure 5. The field dependency of the conductivity will result in a reduction of the highest field strengths by pushing more of the stress into the lower field region, resulting in a more even field distribution through the cable insulation. This will also influence the space charge generation throughout the cable insulation both with and without a temperature gradient. For the higher temperature gradients, a strong field dependency of the conductivity is beneficial as it results in less space charge accumulation and thus a reduction in the space charge induced field.
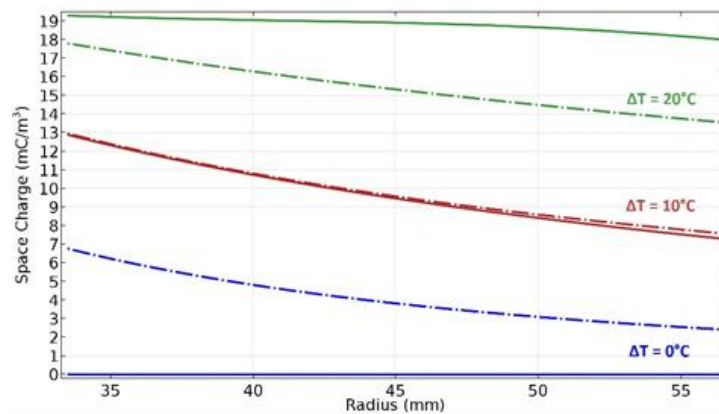
Figure 5. Space charge distribution at steady-state DC with (dotted line) and without field dependency (solid line) of the conductivity for different temperature gradients ΔT.

Directly after a polarity reversal, the space charge will give a contribution to the initially capacitive field distribution. In Figure 6, the field directly after polarity reversal when switching from a steady-state DC field is shown. For ΔT = 20 °C, the field at inner semi-conductor is around 40% higher than the capacitive field (solid line for ΔT = 0 °C) in the case of a field independent conductivity (β = 0), while for a field dependency β = 0.03, the increase in field compared to the capacitive field is about 25%.

Thus, a temperature gradient over any electrical insulation material will give a space charge accumulation, where the particular distribution will be determined by temperature variation and field dependency of the material. To avoid unfortunate field distributions in an extruded polymeric HVDC cable, limitations on maximum ΔT applies, typically 10-15 °C [1].
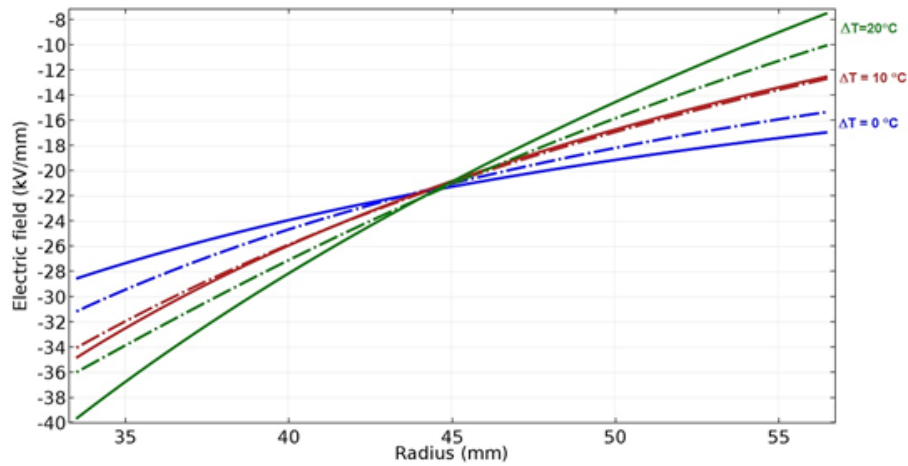
Figure 6. Electric field directly after polarity reversal from steady-state DC for different temperature gradients ΔT with (dotted line) and without field dependency (solid line) of the conductivity.

Simplified cable joint

The effects that the above-discussed phenomena might cause in a cable joint were studied by a simple FEM-model in COMSOL Multiphysics®. The design, showed in Figure 7a, is based on an up-scaled version of a 145 kV AC joint. Although the model does not represent an actual HVDC cable joint, it serves well to investigate the effect of interfaces and temperature distribution in a cable joint at DC stress. The properties of the XLPE insulation is the same as the previously studied cable model while the joint insulation consists of EPDM with conductivity $\sigma_{EPDM}(T, E) = 10^{-15} e^{0.02T + 0.05E}$ S/m. The temperature at the outside of the cable and cable joint was set to 20 °C while varying the conductor temperature to create a ΔT between 0 and 30 °C. Considering the cable joint in a cylindrical coordinate system, the cable is axisymmetric around the z-axis, rendering a two-dimensional model sufficient to represent the joint. Similarly as for the cable model discussed above, a heat transfer problem is solved in a preliminary study step, before the electric potential is solved with conductivities determined by the temperature distribution.

(a)

(b)
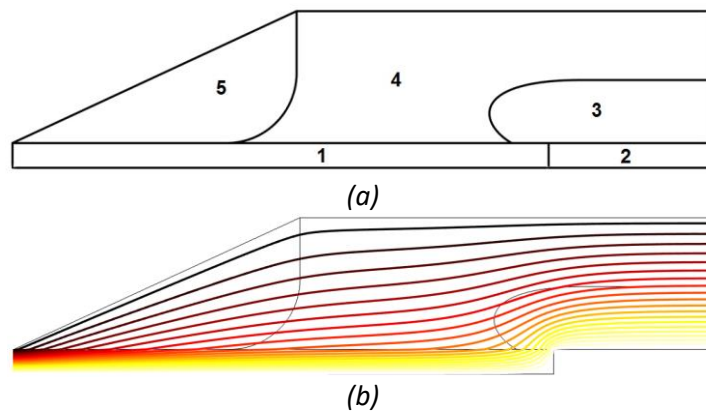
Figure 7. a) Modelled cable joint; 1 – XLPE cable insulation, 2 – metallic connector, 3- inner deflector (rubber material), 4 – joint insulation (EPDM) and 5 – outer deflector. The cable is the same as described in the cable model. b) Temperature distribution in the joint with a temperature gradient of 15 °C.

The normalised electric field distribution at DC stress along the interface for different temperature gradients is shown in Figure 8. As might be expected, a higher field strength is observed around the outer and inner deflectors and a lower field in-between. The higher the temperature gradient, the more the field is concentrated around the

outer deflector. This is due to the temperature dependency of the conductivity and the temperature being higher at the interface closer to the inner deflector than the outer deflector. This will push the DC stress towards the outer deflector. An increase in the tangential field at the interface is undesirable as the breakdown strength of interfaces decreases with increasing temperature [7].
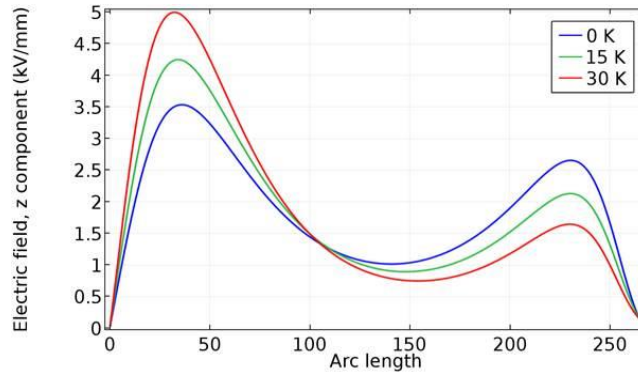
Figure 8. Normalised electric field strength along the XLPE-EPDM interface from the outer to the inner deflector at various temperature gradients.
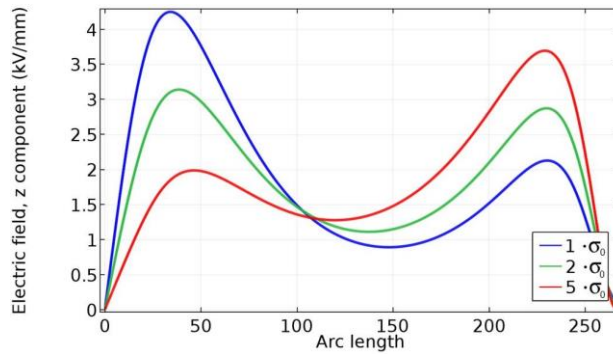
(a)
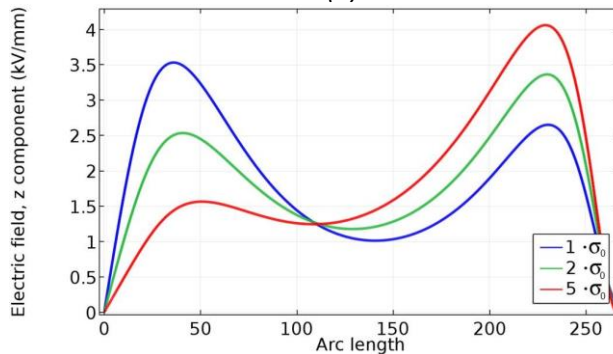
(b)

Figure 9. Normalised electric field strength along the XLPE-EPDM interface for a) $\Delta T = 0\ °C$ and b) $\Delta T = 15\ °C$ for different values of σ_0 for the EPDM conductivity.

Ideally, an interfacial field strength should be temperature independent. In this design, an increased conductivity of the joint insulation can reduce the temperature dependency of the interfacial field strength. Using COMSOL Multiphysics®, the influence of different conductivities of the joint insulation was studied. In Figure 9, the normalised interfacial electric strengths for some of the conductivities studied in case of no-load and full-load ($\Delta T =$

15 °C) are shown. Here, increasing the conductivity by a factor of two compared the original conductivity yields an interfacial field distribution that is almost temperature independent.

An alternative, which is not studied here, is the use of a field grading material (FGM) along the interface between the two deflectors. As a FGM has a very strong field and temperature dependency, the field strength along the interface would be more even and give an effective field grading. However, a FGM will add triple junctions to the design that would have to be handled when designing the cable joint.

Conclusions

The conductivity of the electrical insulation depends strongly on the temperature, and the field distribution in a HVDC cable system is time and load dependent. Thus, the field has to be calculated for all stages and load situations that might occur, from switching the voltage on, no- and full-load and, if relevant for the HVDC system considered, polarity reversals. In addition, switching impulses and, where relevant, lightning impulses superimposed on a DC need to be considered for both no- and full-loaded cables.

For a cable, the initial field distribution when switching the HVDC voltage on can be found analytically using the capacitive field distribution. For the field distribution at any other stages, the conductivity with its field and temperature dependency need to be considered. The resistive field distribution will lead to an increasing space charge build-up with increasing temperature gradient over the cable. However, the field dependency of the insulation material is beneficial as it reduces the maximum fields. Thus, for a cable, the space charge build up and resulting electrical field distribution should not be of concern as long as the temperature gradient over the insulation is controlled and limited to typically 10-15 °C.

The design challenge when it comes to HVDC cables and their accessories is related to the inevitable interfaces that will be present at a cable joint or termination. The permittivity of insulation materials normally differs little, but the conductivities can vary over several decades in addition to having a strong temperature dependency. For AC cable accessory designs from the lower to the highest voltages, geometric and capacitive field grading and FGM are used to control the electric field. For HVDC, the initially field distribution will be similar to that at AC, but after a transition period, a conductive DC field distribution is established that is strongly temperature dependent. However, taking the possible temperature distributions into account, carefully tuning of the conductivities can give designs that works within the expected temperature ranges. Also for HVDC designs, a FGM with a strong field dependency can be used beneficially.

References

[1]   G. Mazzanti *et al.*, *Extruded Cables for High-Voltage Direct-Current Transmission*. IEEE Press, Wiley, 2013.

[2]   F. Mauseth, E. Ildstad, M. Selsjord, and R. Hegerberg, "Quality control of extruded HVDC cables: Low frequency endurance testing of model cables with contaminations," presented at the 2010 International Conference on High Voltage Engineering and Application (ICHVE), New Orleans, USA, 2010.

[3]   T. Maeno, "Protabel space charge measurement system using the pulsed electrostatic method," *IEEE Trans. Dielectr. Electr. Insul.,* vol. 10, no. 2, 2003.

[4]   P. Alto, "DC Cable Systems with Extruded Dielectrics," EPRI, December 2004.

[5]   F. H. Kreuger, *Industrial High DC Voltage*. Delft University Press, 1995.

[6]   Z. Zheng and S. Boggs, "Defect Tolerance of Solid Dielectric Transmission Class Cable". *IEEE Electr.Insul. Mag.* vol. 10, no. 2, 2005.

[7]   N. Amyot and D. Fournier, "Influence of thermal cycling on the cable-joint interfacial pressure," in *IEEE Int. l Conf. on Solid Dielectr.,* Eindhoven, The Netherlands, 2011.

Frank Mauseth received his MSc degree in Electrical Engineering from Delft University of Technology, The Netherlands, in 2001. Since then he has been with the Norwegian University of

Science and Technology (NTNU) in Trondheim, Norway, where he received his PhD degree in 2007 and is now an Associate Professor. Main fields of interest are high voltage insulation materials and systems, measurement methods and testing. Is currently active within the IEEE DEIS TC "HVDC Cable Systems" and CIGRÉ WG D1.48.

Hallvar Haugdal received his MSc degree in Electric Power Engineering from the Norwegian University of Science and Technology (NTNU) in Trondheim, Norway, in 2016. Since then he has been working as a Scientific Assistant at NTNU, where he has participated in various projects on Electrical Machine Design and FEM simulations, in addition to educational work in the same fields.